Computational Study of Graphene FETs (GFETs) as Room-Temperature Terahertz Emitter

Wenshen Li[1], Shi Dong[1], He Wang[2], Jinyu Zhang[1*], Yan Wang[1], and Zhiping Yu[1]
[1]Institute of Microelectronics, Tsinghua University, Beijing 100084, China
[2]Department of Electrical Engineering, Stanford University, California 94305, USA
*Email: zhangjinyu@tsinghua.edu.cn

***Abstract*—The effect of electron scattering on the plasma-wave instability in the channel of GFETs has been studied through solving the governing hydrodynamic (HD) equations numerically, which are based on the linear energy-momentum dispersion, i.e., Dirac cone, of graphene [1]. It is revealed that there exists a critical scattering strength determined by the carrier mobility and channel length, above which the instability cannot be sustained. While analytical solution can only be obtained under the dissipationless condition, numerical calculation is conducted considering the scattering term. We conclude that the realization of room temperature terahertz emitter is possible in GFETs as long as careful device design and high quality graphene channel are achieved.**

I. Introduction

The generation of terahertz radiation through plasma-wave instability in field-effect transistors (FETs) has long been proposed by Dyakonov and Shur (D-S) if ballistic carrier transport is assumed [2]. The plasma-wave instability occurs due to the wave velocity difference caused by the DC drain current, together with the asymmetric AC boundary condition arising from the gate-source voltage bias and drain-source current bias. Utilizing the instability, room temperature terahertz emitters can be realized. In the real world, however, there are always some wave magnitude damping mechanisms in the channel which reduces the instability, among which the carrier scattering plays the biggest role. Previous study has calculated the effect of scattering on the D-S instability [3] and the analysis on two of the experimental works [4], [5] has shown the evidence of insufficient mobility for plasma wave generation in the III-V channel materials used in the real devices [6]. Thus the exploration of D-S instability in high mobility channel materials is strongly desirable.

Graphene is a single-layered material with excellent electronic transport properties. Its honeycomb crystal lattice gives rise to its high sample quality and the potential for ultra-high room temperature mobility [7]. In encapsulated graphene samples, room temperature mobility exceeding $\sim 100,000 \mathrm{cm}^2/\mathrm{V}\cdot\mathrm{s}$ is achieved. The extraordinary mobility and the ease for gate control makes graphene a strong candidate as the channel material for the D-S FETs. However, because of the linear band profile in graphene, constant effective mass can not be introduced as in the case of parabolic band. As a result, the hydrodynamic equations describing the dynamic of electrons in the graphene channel are different from those used in the initial proposal of D-S theory. The immediate consequence of this bandstructure difference is a smaller wave velocity mismatch at the drain end of the channel under same drain current, which results in a smaller growth rate of the plasma-wave amplitude in the ballistic case [1], leading to a rather dim projection of using GFETs for THz generation through D-S instability. When scattering is considered, however, the excellent mobility in graphene may offer a compensation for the smaller instability effect and may lead to promising realization of room temperature terahertz emitters.

In this study, we analyze the effect of scattering on the D-S plasma-wave instability in GFET through numerical methods and discuss the feasibility of utilizing GFETs as room temperature terahertz emitters. We show that the plasma-wave instability is indeed reduced by the scattering effect and we calculate the critical scattering strength above which no instability occurs. Based on the critical scattering strength, we compute the room temperature mobility requirement and find it achievable in high quality graphene samples.

II. Method

The form of the HD (hydrodynamic) equations describing the dynamic of the electrons in gated-graphene is adopted from [1], which are derived from the Boltzmann transport equation taking the linear energy-momentum dispersion into account and assuming a displaced Fermi-Dirac (F-D) distribution $f = \left\{\exp\left[\frac{\varepsilon(\mathbf{k})-\hbar\mathbf{k}\cdot\mathbf{v}-\mu}{k_BT}\right]+1\right\}^{-1}$ with $\mathbf{v}$ the electron drift velocity and μ the chemical potential. The electron sheet density n and its flow density $\mathbf{j}$ can be expressed by [1]

$$n = \frac{n_{v=0}}{[1-v^2/v_F^2]^{3/2}}, \quad (1)$$

$$\mathbf{j} = n\mathbf{v} \quad (2)$$

where $n_{v=0}$ is the static density (i.e. the density when the drift velocity is zero) solely determined by μ (w.r.t. the Dirac point where $\mu = 0$) and T: $n_{v=0} = \frac{2(k_BT)^2}{\pi\hbar^2v_F^2}\int_0^\infty \frac{tdt}{1+e^{t-\mu/k_BT}}$. Utilizing the gradual channel approximation, the hydrodynamic equations governing $n(x,t)$ and $v(x,t)$ in the 1D channel read

$$\frac{\partial n}{\partial t} + \frac{\partial (nv)}{\partial x} = 0 \quad (3)$$

$$\frac{\partial v}{\partial t}[1+\theta] + v\frac{\partial v}{\partial x}[(3-4\xi)-\theta] + \frac{\partial n}{n\partial x}{s_0}'^2 = -\frac{v}{\tau_p} \quad (4)$$

where $\xi = F_1(\frac{\mu}{k_BT})^2/2F_2(\frac{\mu}{k_BT})F_0(\frac{\mu}{k_BT})$ and $\theta = \frac{\beta^2(5-6\xi)}{1-\beta^2}$ are dimensionless coefficients determined by μ/k_BT and the dimensionless drift velocity $\beta = v/v_F$ ($F_j(x) = \frac{1}{\Gamma(j+1)}\int_0^\infty \frac{t^j}{e^{t-x}+1}dt$ is the Fermi-Dirac intergral of order j

978-1-4673-7860-4/15/$31.00 ©2015 IEEE

($j = 0, 1, 2$)). s_0' is another coefficient representing the plasma-wave velocity

$$s_0' = v_F \sqrt{\frac{2\xi}{3}\left(1 - \beta^2 + \frac{e^2\langle\varepsilon^{-1}\rangle}{C_{ox}}\right)} \tag{5}$$

where C_{ox} is the gate capacitance and $\langle\varepsilon^{-1}\rangle = 2k_BT\ln(1+e^{\mu/k_BT})/\pi\hbar^2 v_F^2\sqrt{1-\beta^2}$ is the density of inverse energy [1]. In order to examine the effect of scattering, a dissipative term $-v/\tau_p$ is added to the right hand side of the Euler equation (Eq. 4) with τ_p the effective momentum relaxation time.

Obviously, the HD equations in gated-graphene has more complex form than those in parabolic band semiconductors as used for the original D-S instability proposal. More importantly, Eqs. (3-4) are not closed for the two variables n and v to be solved, i.e., there are more variables than equations. Specifically, the coefficients ξ, θ and s_0' all depend on the chemical potential μ (the temperature T can be taken as a constant), which can not be explicitly expressed in the two variables n and v. In principle, the heat-transfer equation as shown in [1] should be included to fully characterize the problem. However, the involvement of such an equation will pose difficulty on setting the boundary condition for the energy density, which is neither set directly by the DC bias nor easily measured.

Therefore, we limit our discussion based only on Eqs. (3-4). Overall, two variables: electron sheet density, n, and electron drift velocity, v, are to be solved with boundary conditions

$$n(0,t) = \text{const}, \tag{6}$$
$$j(L,t) = n(L,t)v(L,t) = j_0 = \text{const} \tag{7}$$

where L is the channel length. For dissipationless case as discussed in [1], the lack of a third equation for the problem does not introduce any difficulty, since the steady-state distribution of all the variables and coefficients are constant along the channel, thus ξ, θ and s_0' can be taken as constants in Eq. (4) when doing time-dependent analysis. However, in our case, the dissipative term $-v/\tau_p$ in Eq. (4) leads to non-uniform distribution of the variables n and v as well as a position-dependent μ and the coefficients associated with it, making analytical treatment impossible in both the steady-state and the time-dependent analysis.

We use two different methods to tackle this issue. The first one is to treat the coefficients ξ, θ and s_0' as of constant values, as long as the dimensionless scattering strength measured by

$$\gamma = \frac{L}{v_F\tau_p} \tag{8}$$

is small.

The second method utilizes the asymptotic form for the Fermi-Dirac integrals to express μ as function of the solution variables n and v. When $x \to \infty$, $F_0(x) \to x$, $F_1(x) \to \frac{x^2}{2}$, $F_2(x) \to \frac{x^3}{6}$. Using these asymptotic expressions, ξ [1] and $\langle\varepsilon^{-1}\rangle$ can be written as functions of n and v under the condition of $\mu/k_BT \gg 1$

$$\xi = \frac{3}{4} - \frac{3n_T}{2n_{v=0}}, \tag{9}$$
$$\langle\varepsilon^{-1}\rangle = \frac{2\sqrt{n}}{\sqrt{\pi}\hbar v_F}(1-\beta^2)^{1/4} \tag{10}$$

where n_T is the density of thermally activated electrons at $\mu = 0$.

In this way, coefficients ξ, θ and s_0' become n, v dependent only and Eqs. (3-4) are now enough for solving n and v. The steady-state solution $n_0(x)$ and $v_0(x)$ are easily obtained by setting the time derivatives to be zero in Eqs. (3-4). Note that this method requires $\mu/k_BT \gg 1$. It is found that the error is less than $\sim$10% for $\mu/k_BT \geq 7$.

As in [2], the time-dependent solutions are expressed as the sum of the steady-state solution and time-harmonic perturbations

$$n(x,t) = n_0(x) + n_1(x)\exp(-i\omega t), \tag{11}$$
$$v(x,t) = v_0(x) + v_1(x)\exp(-i\omega t), \tag{12}$$

The real part ω' of the complex angular frequency $\omega = \omega' + i\omega''$ is related to the oscillation frequency of the plasma-wave with $\omega' = 2\pi f$. The imaginary part ω'' is the rate of increment of the plasma-wave amplitude (wave increment). The goal is to find ω'', which is obtained from our simulation program modified from our previous work [6] solving for the time evolution of the initial perturbation on n and v

$$n_1(x) = A_0\sin(\pi x/L), \tag{13}$$
$$v_1(x) = 0 \tag{14}$$

In order to compare the simulation results to some analytical solutions, the low scattering limits are derived. Under $\beta_0 \ll 1$, $\gamma \ll 1$, the wave increment can be analytically calculated from Eqs. (3-4)

$$\omega'' = \frac{v_F}{L}\left[2\beta_0(1-\xi) - \frac{\gamma}{2}\right] \tag{15}$$

We define the critical scattering strength γ_{cr} to be the maximum scattering strength above which no plasma-wave instability occurs, i.e., the wave increment ω'' becomes zero. It follows that

$$\gamma_{cr} = 4\beta_0(1-\xi) \tag{16}$$

III. Results and Discussion

For the simulated GFET, a typical gate capacitance $C_{ox} = 4.4\times10^{-7}\mathrm{F/cm^2}$ ($EOT = 7.8\mathrm{nm}$) is assumed, e.g., with a dielectric constant of 10 and a thickness of 20nm. Room temperature condition ($T = 300K$) is assumed. With the use of dimensionless parameters γ and $(L/v_F)\omega''$, the results apply to arbitrary channel length.

Fig. 1 shows the effect of different scattering strength γ on the wave increment ω'' for a fixed chemical potential $\mu = 7k_BT$ at the source end, corresponding to a static electron sheet density of $\sim2.6\times10^{12}\mathrm{cm^{-2}}$. The wave increment is plotted against the normalized drift velocity at the source end which represents the current bias applied to the drain. The black solid line is the theoretical result with no scattering [1], which is well-matched by our simulation results (black

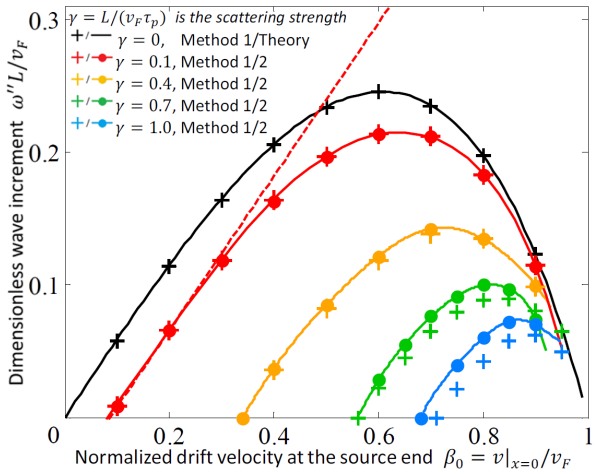

Fig. 1. Effect of different scattering strength γ on wave increment ω'' for fixed source end chemical potential of $\mu = 7k_BT$. Dotted line is the low scattering limit (15) for $\gamma = 0.1$ which is well-matched for small β_0 values. Crosses and connected dots represent simulation results based on approximation method 1 and 2, respectively. The theoretically result in [1] for $\gamma = 0$ is matched by our simulation results. The discrepancy between method 1 and 2 becomes appreciable only when $\gamma > 0.4$, indicating that method 1 is a good approximation although crude in nature. The error arising from the asymptotic expressions (Eqs. 9-10) is already excluded for a better comparison of the two methods.

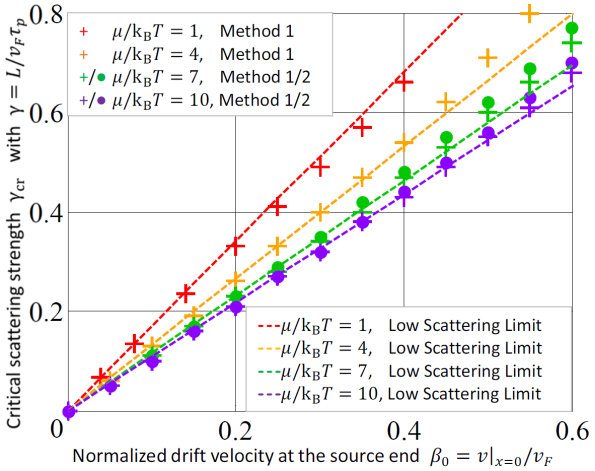

Fig. 2. The critical value of the scattering strength γ_{cr} vs. the normalized drift velocity β_0 for different values of source end chemical potential. Method 2 is used when $\mu/k_BT = 7, 10$, respectively. Straight dotted lines are the low scattering limit (Eq.16), which match well with the simulated γ_{cr} at low γ_0, even at higher γ_0, rendering Eq. (16) a good expression for estimating γ_{cr}.

crosses), indicating the correctness of our simulation program. For $\gamma > 0$, two different approximation methods are used as indicated in the previous section. As expected, the wave increment decreases as the scattering becomes stronger. Superior behavior is observed as graphene does not incur the choking effect at large drain current bias (reflected by $\beta_0 = v|_{x=0}/v_F$) as in conventional semiconductor FETs [3], [8]. Also, our theoretical prediction Eq. (15) for low scattering limit is well-matched for $\gamma = 0.1$. Note that the discrepancy between approximation methods 1 and 2 is becomes appreciable only for $\gamma > 0.4$, where the steady-state distribution of the coefficients and variables deviates from uniform distribution to a non-negligible extent due to strong scattering effect.

The critical scattering strength γ_{cr} defined before can also be simulated for each drain current bias. Such threshold for the instability is computed in a typical bias condition, e.g., $\beta_0 \leq 0.6$ as shown in Fig. 2. It can be seen that small source end chemical potential μ and high source end drift velocity β_0 allows for high γ_{cr}, but the differences incurred by μ is small. Again, the low scattering limit (Eq. 16) is well-matched for small γ value. Surprisingly, a good match is observed even for large γ, rendering Eq. (16) a good expression for estimating γ_{cr}.

Based on the simulated critical scattering strength, the room temperature mobility requirement and the design rule of the channel length for desired oscillation frequency can be computed. In graphene, the electron mobility (we use μ_m to avoid confusion with the chemical potential μ) is related to τ_p via $\mu_m = ev_F^2\tau_p/E_F$ [9], where E_F is the Fermi energy. After using the zero temperature expression $n = E_F^2/\pi(\hbar v_F)^2$, we get the expression for μ_m

$$\mu_m = \frac{ev_F}{\hbar\sqrt{\pi}\sqrt{n}}\tau_p \tag{17}$$

Eq. (17) can be cast to another form by using the definition for the scattering strength (Eq. 8)

$$\mu_m = \left(\frac{e}{\hbar\sqrt{\pi}\sqrt{n}}\right)\frac{L}{\gamma} \tag{18}$$

Thus, for a fixed scattering strength γ, the mobility requirement is proportional to the channel length. The oscillation frequency f can not be analytically expressed once the scattering is taken into account. We can estimate the frequency using the expression in the ballistic case [1]

$$f = \frac{m}{4L}\frac{s_0'^2 - v_0^2(3-4\xi-\theta)}{\sqrt{s_0'^2(1+\theta)+v_0^2(2\xi-1+\theta)^2}}\ (m = 1, 2, 3, \cdots) \tag{19}$$

where m denotes the mode number. Normally, the steady-state drift velocity v_0 is set no bigger than $0.6v_F$, thus the v_0^2 terms in Eq. (19) can be neglected for a rough, yet simpler estimation of the oscillation frequency of the first mode

$$f \simeq \frac{s_0'}{4L} \tag{20}$$

As for the wave velocity coefficient s_0', we refer to Eq. (5) and do some simplifications as such: under a typical density of $n \sim 10^{12}/\mathrm{cm}^2$, ξ is around 0.7, so $2\xi/3(1-\beta^2)$ is estimated as 0.4; $\langle\varepsilon^{-1}\rangle$ can be estimated by taking $\ln(1+e^{\mu/k_BT})$ to be μ/k_BT in its detailed expression. We thus arrive at

$$s_0' \simeq v_F\sqrt{0.4 + \frac{3}{C_{ox}(\times 10^{-7}\mathrm{F/cm}^2)}\cdot\left(\frac{\mu}{k_BT}\right)} \tag{21}$$

From Fig. 2, the value of the critical scattering strength γ_{cr} is evaluated roughly as 0.5 from the current bias of $\beta_0 \sim 0.5$ where the largest wave increment under no scattering is

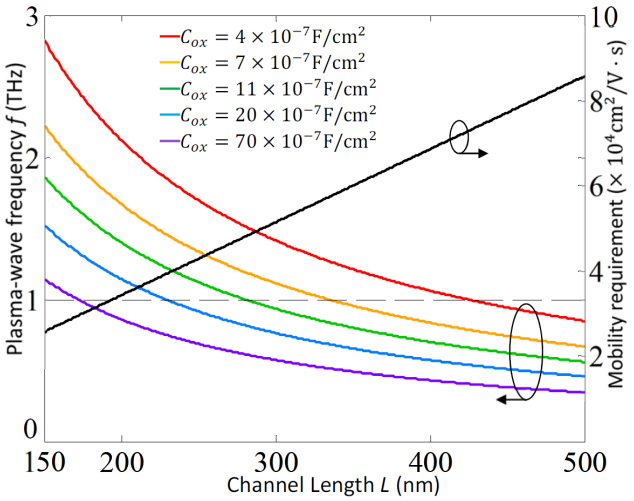

Fig. 3. Dependence of mobility requirement and plasma-wave frequency on channel length, under typical sheet density of $n = 10^{12}\mathrm{cm}^{-2}$. The required mobility increases with the increase of L, while the plasma-wave frequency decreases. Increasing the gate capacitance reduces f at fixed channel length. 1THz operation is indicated by the dash line.

located. Based on this value, the dependence of the required mobility and the plasma-wave frequency on the channel length is computed and shown in Fig. 3, assuming a typical electron sheet density $n = 10^{12}\mathrm{cm}^{-2}$. The 1 THz operation condition is marked by the dash line. It can be seen from Fig. 3 and the expression for s_0' that for a fixed channel length, the plasma-wave frequency can be tuned by changing the gate capacitance and the chemical potential μ, which is in turn set by the gate-source voltage bias in a way where the quantum capacitance plays a non-negligible role. Under the condition of a fixed electron sheet density in Fig. 3, a larger C_{ox} will lead to a shorter channel length at a fixed operation frequency, allowing for lower room temperature mobility requirement.

A numerical example can be given. For a device with $C_{ox} \sim 4\times10^{-6}\mathrm{F/cm}^2$ ($EOT = 0.86\mathrm{nm}$) and $n = 10^{12}\mathrm{cm}^{-2}$, 1 THz plasma-wave frequency can be achieved by having the channel length to be $180\mathrm{nm}$, which means a room temperature mobility requirement of $\sim 32,000\mathrm{cm}^2/\mathrm{V}\cdot\mathrm{s}$. As discussed above, the mobility requirement can be lessened by shortening the channel length. But it will also lead to a higher frequency unless larger C_{ox} is simultaneously achieved.

IV. Conclusions

The hydrodynamic equations in graphene with the scattering term considered has been numerically studied in order to investigate the effect of scattering on the D-S plasma-wave instability in GFETs, which has the potential for realizing room temperature solid-state terahertz emitters. We show that the plasma-wave instability is indeed reduced by the scattering effect and we calculate the critical scattering strength above which no instability will occur. The feasibility of GFETs-based room temperature terahertz emitters has been discussed by numerical examples. We found the mobility requirement to be proportional to and the plasma-wave frequency inversely proportional to the channel length. The frequency can be further adjusted by the gate capacitance as well as the gate-source voltage bias. Using the calculated critical scattering strength, we found the required room temperature mobility to be around several $10,000\mathrm{cm}^2/\mathrm{V}\cdot\mathrm{s}$ for the plasma-wave frequency of 1 THz. Even though the requirement is high, it is achievable in high quality graphene samples due to graphene's extraordinary transport properties.

Acknowledgment

This work was supported in part by the National 973 Program under Grant 2011CBA00600 and Grant 2011CB933004, in part by the Important National Science and Technology Special Projects under Grant 2011ZX02707, all in China.

References

[1] D. Svintsov, V. Vyurkov, V. Ryzhii, and T. Otsuji, "Hydrodynamic electron transport and nonlinear waves in graphene," *Physical Review B*, vol. 88, no. 24, p. 245444, 2013.

[2] M. Dyakonov and M. Shur, "Shallow water analogy for a ballistic field effect transistor: New mechanism of plasma wave generation by dc current," *Physical review letters*, vol. 71, no. 15, p. 2465, 1993.

[3] M. Cheremisin, M. Dyakonov, M. Shur, and G. Samsonidze, "Influence of electron scattering on current instability in field effect transistors," *Solid-State Electronics*, vol. 42, no. 9, pp. 1737–1742, 1998.

[4] W. Knap, J. Lusakowski, T. Parenty, S. Bollaert, A. Cappy, V. Popov, and M. Shur, "Terahertz emission by plasma waves in 60 nm gate high electron mobility transistors," *Applied Physics Letters*, vol. 84, no. 13, pp. 2331–2333, 2004.

[5] T. Onishi, T. Tanigawa, and S. Takigawa, "High power terahertz emission from a single gate algan/gan field effect transistor with periodic ohmic contacts for plasmon coupling," *Applied Physics Letters*, vol. 97, no. 9, p. 092117, 2010.

[6] H. Wang, W. Li, J. Zhang, Y. Wang, and Z. Yu, "The role of electron viscosity on plasma-wave instability in hemts," in *Simulation of Semiconductor Processes and Devices (SISPAD), 2014 International Conference on*. IEEE, 2014, pp. 177–180.

[7] S. Morozov, K. Novoselov, M. Katsnelson, F. Schedin, D. Elias, J. Jaszczak, and A. Geim, "Giant intrinsic carrier mobilities in graphene and its bilayer," *Physical review letters*, vol. 100, no. 1, p. 016602, 2008.

[8] M. Dyakonov and M. Shur, "Choking of electron flow: A mechanism of current saturation in field-effect transistors," *Physical Review B*, vol. 51, no. 20, p. 14341, 1995.

[9] E. Hwang and S. D. Sarma, "Acoustic phonon scattering limited carrier mobility in two-dimensional extrinsic graphene," *Physical Review B*, vol. 77, no. 11, p. 115449, 2008.